REVIEW

OPEN

New views on three-dimensional imaging technologies for glaucoma: an overview

Maria A. Guzman Aparicio[a,b] *and Teresa C. Chen*[a,b]

Purpose of review
To summarize the literature on three-dimensional (3D) technological advances in ophthalmology, the quantitative methods associated with this, and their improved ability to help detect glaucoma disease progression.

Recent findings
Improvements in measuring glaucomatous structural changes are the result of dual innovations in optical coherence tomography (OCT) imaging technology and in associated quantitative software.

Summary
Compared with two-dimensional (2D) OCT parameters, newer 3D parameters provide more data and fewer artifacts.

Keywords
glaucoma, imaging, optical coherence tomography angiography, optical coherence tomography, software upgrades

INTRODUCTION

Glaucoma is a chronic optic neuropathy, for which there is no cure. Early detection is the key to preserving vision as appropriate treatment can delay progression and prevent irreversible blindness. Historically, the diagnosis of perimetric glaucoma was made when a person had already lost up to 40% of their retinal ganglion cells (RGC). However, there is now a shift towards detecting glaucomatous structural changes before visual field loss as results of the Ocular Hypertension Treatment Study and advances in imaging have shown that changes in structural testing [i.e. disc photography and optical coherence tomography (OCT)] can occur before visual field changes. With OCT technology, these changes include retinal nerve fiber layer (RNFL) thinning, neuroretinal rim tissue thinning, and macular ganglion cell layer thinning. Imaging now has the capability of providing doctors with more data and fewer artifacts, or fewer clinically unusable scans. Additionally, OCT provides data on the surrounding peripapillary vasculature and can also visualize the lamina cribrosa, giving insights into the vascular and mechanical theories of glaucoma. This review will summarize best clinical three-dimensional (3D) imaging technologies and associated 3D volumetric analyses, which will enable us to diagnose and detect 3D glaucomatous structural changes sooner, ultimately enabling earlier treatment and vision preservation.

TECHNOLOGY OVERVIEW: SPECTRAL DOMAIN AND SWEPT SOURCE OPTICAL COHERENCE TOMOGRAPHY

OCT is the most commonly used, noninvasive, in-vivo 3D imaging technology currently used in clinics. It has become a foundational part of the evaluation of glaucoma and retinal diseases, and it can help to objectively quantify disease progression. Images in OCT can be translated into one-dimensional (1D) units of data or length or A-scans. Many

[a]Harvard Medical School and [b]Department of Ophthalmology, Massachusetts Eye and Ear Infirmary, Glaucoma Service, Boston, Massachusetts, USA

Correspondence to Teresa C. Chen, MD, Massachusetts Eye and Ear Infirmary, Glaucoma Service, 243 Charles Street, Boston, MA 02114, USA. Tel: +1 617 573 3674; fax: +1 617 573 3707;
e-mail: teresa_chen@meei.harvard.edu

Curr Opin Ophthalmol 2022, 33:103–111

DOI:10.1097/ICU.0000000000000828

KEY POINTS

- The 2D RNFL thickness measurements are the result of a single B-scan. The presence of artifacts in one B-scan can lead to a wrong diagnosis and incorrect treatment plans.
- Compared with SD-OCT, SS-OCT has faster scan speeds and better depth penetration, enabling better visualization of deeper structures, such as the lamina cribrosa and choroid.
- High-density 3D volumetric analysis affords more data and fewer unusable scans and would improve glaucoma care in the future. Such newer parameters may include RNFL volume, MDB neuroretinal rim thickness, peripapillary retinal volume, and GCC volume.

A-scans combined together create B-scans, which are two-dimensional (2D) cross-sectional images. Volumetric or 3D images are created when B-scans are combined. During the transition of 2D to 3D imaging of the eye, OCT became an indispensable part of clinical practice.

During the past decades, OCT technology has been continuously evolving. First described in 1991, time domain OCT laid the groundwork for in-vivo 2D imaging of the eye [1]. In 2003, 3D volumetric imaging of the eye with video-rate spectral domain OCT (SD-OCT) became possible [2]. Faster-scan speeds allowed for unprecedented video imaging of the posterior pole. Fourier domain OCT and SD-OCT are different terms for the same technology, whose advancement allowed for better sensitivity and higher resolutions [3,4]. Video-rate SD-OCT propelled the use of OCT machines in almost every ophthalmology office, utilizing a spectrometer and light source wavelengths ranging from 820 to 870 nm for the RTVue and iVue (Optovue Inc., Fremont, California, USA), the Cirrus (Carl Zeiss Meditec, Inc., Dublin, California, USA), and the Spectralis (Heidelberg Engineering, GmbH, Heidelberg, Germany) [5].

Around the same time, another technology advancement called swept source OCT (SS-OCT) was developed [6–8]. Optical frequency domain imaging, or SS-OCT, was not Food and Drug Administration (FDA) approved for clinical use until 2016 and is not as commonly used in ophthalmology clinics as SD-OCT. However, compared with SD-OCT, SS-OCT has faster-scan speeds and greater depth penetration, allowing for scanning of larger areas and deeper layers. SS-OCT uses a laser light with a center wavelength of approximately 1050 nm [9–11,12▪▪,13,14].

Variations of SD-OCT technology include enhanced-depth imaging (EDI), which simply focuses imaging to more posterior structures. Other enhancements may include adaptative optics, which reduces the aberrations caused by the lens in the eye, providing better resolution with reduction of artifacts [15▪,16,17].

Another added feature for SD-OCT and SS-OCT technologies is OCT angiography (OCTA), which visualizes blood vessels [18▪▪]. Although SD-OCT has the ability to measure blood flow [19], most commercially available OCTA software does not quantify blood flow but simply visualizes the presence or absence of blood vessels. With current software packages, the 3D vascular network in the eye can be visualized without fluorescein angiography or dye, and metrics, such as vessel density can be quantified. With the advent of OCT, the use of invasive fluorescein angiography has been vastly reduced. With current OCTA software, serial images in time are compared, and image differences are attributed to the presence of moving blood cells, which indicate the presence of blood vessels. Therefore, the structural presence of blood vessels can be mapped for different regions, such as the retinal surface, the radial peripapillary capillary network, and the intermediate and deep capillary plexus [20–22,23▪].

This review will focus on structural imaging and not vascular imaging as normative databases are only available for structural and not OCTA parameters. In addition, structural measurements are currently more reliable than OCTA data.

FUTURE CLINICAL APPLICATIONS: BEYOND THE RETINAL NERVE FIBER LAYER

Although OCT technology now allows for 3D volumetric imaging of the eye, its full potential is limited by commercially available software, which does not fully analyze the volumetric data obtained by the machines. Therefore, software advances with 3D data analysis are needed to maximize the potential of SD-OCT and SS-OCT technology. Currently, the most commonly used glaucoma parameter is peripapillary RNFL thickness [3]. However, we need to move beyond the RNFL. Future regions of interest that need to be targeted for better glaucoma diagnosis and monitoring of disease progression are not only just the RNFL but also the optic nerve, the peripapillary region, and the macula.

STARTING WITH RETINAL NERVE FIBER LAYER THICKNESS: TWO-DIMENSIONAL IMAGING

The peripapillary RNFL thickness parameter is the most commonly used, commercially available

glaucoma parameter in clinical practice [3], and these 2D RNFL thickness measurements are the result of a single B-scan. Thinning of the RNFL is associated with glaucoma. However, the greatest limitation of the RNFL thickness measurement is that its OCT measurements may be inaccurate because of artifacts in 19.9–46.3% of scans [24,25,26▪▪,27▪,28]. In an analysis of 2313 scans from 1188 patients, Liu *et al.* defined 12 types of artifacts, which can be caused by poor data acquisition, inaccurate software analysis, or patient ocular disorder [28]. Moreover, the RNFL thickness parameter has high false-positive rates of 26.2–39% (i.e. 'red disease' when the OCT machine suggests incorrectly that the patient has glaucoma), in patients with longer axial lengths and smaller disc areas [29]. Additionally, RNFL measurement errors and artifacts are more commonly seen in glaucoma patients [25,29], as glaucoma causes not only RNFL thinning but also RNFL reflectivity loss. As the less reflective glaucomatous RNFL is harder to distinguish from the underlying plexiform layer, segmentation of the posterior RNFL border may be more difficult and inaccurate. Because of the high-artifact rates seen with peripapillary RNFL thickness measurements, research to develop better ways to more accurately quantify the RNFL in glaucoma is needed.

RETINAL NERVE FIBER LAYER VOLUME: THREE-DIMENSIONAL IMAGING

Peripapillary RNFL volume is perhaps a better future metric for quantifying RNFL tissue in glaucoma than the aforementioned RNFL thickness parameter. In a study by Khoueir *et al.* [30], high-density optic nerve volumetric research scans were used to evaluate the diagnostic capability of SD-OCT peripapillary RNFL volume measurements in a multiethnic group of 113 open-angle glaucoma (OAG) patients and 67 normal participants. Employing a custom-designed MATLAB code, RNFL volume for different-sized annuli were calculated from high-density volume scans centered on the optic nerve head (ONH). This study concluded that overall RNFL volume measurements were lower in OAG patients compared with normal patients. Using different annuli sizes of 1 mm width, the best diagnostic capability was found for the circumpapillary annulus (i.e. RNFL-volume 2.5–3.5), which had an inner diameter of 2.5 mm and an outer diameter of 3.5 mm [area under the receiver operating characteristic curve (AUROC) = 0.955]. Of the eight possible RNFL volume sectors (i.e. for 4 quadrants and 4 octant values), the inferior quadrant had the best diagnostic ability (AUROC = 0.977). These results were then compared with the best diagnostic values for 2D RNFL thickness, which were global (AUROC = 0.959) 0.959) and inferior (AUROC 0.966). Although RNFL volume parameters had similar ability as RNFL thickness to help diagnose glaucoma [30], a complementary RNFL volume paper shows that this same high-density 3D RNFL volume parameter can reduce the percentage of clinically unusable scans in glaucoma patients to 7.5%, lower than the 58.5% of unusable scans for the 2D RNFL thickness scan [31▪▪]. Therefore, this 3D high-density volumetric scan protocol, which takes only a few extra seconds of scan time [30], can achieve improved data accuracy [31▪▪] by reducing the number of unusable scans, which would otherwise require repeat scanning. In summary, RNFL volume measurements have the same diagnostic ability as RNFL thickness measurements but provide more data and fewer unusable scans, which would improve future glaucoma care.

THE OPTIC NERVE: BRUCH'S MEMBRANE OPENING-MINIMUM RIM WIDTH AND THREE-DIMENSIONAL IMAGING

The key feature of old neuroretinal rim measurements is that rim tissue is only quantified if it lies along a 2D flat reference plane, which varies from 120 to 200 μm above and parallel to the retinal pigment epithelium (RPE). According to a review [3], best commercially available rim parameters are global and inferior rim area along this 2D flat reference plane. In contrast, the key feature of new neuroretinal rim measurements is that rim thickness is calculated in 3D space and does not use a 2D mathematically flat reference plane [2]. The earliest commercially available reference plane-independent parameter is the low-density Bruch's membrane opening-minimum rim width (BMO-MRW) parameter, which quantifies 360° of rim tissue in 3D space using the cup surface as the inner rim border and the BMO disc border as the outer rim border. Articles suggest that the BMO-MRW is the same as or better than both RNFL thickness and reference plane-dependent rim area for diagnosing glaucoma and monitoring disease progression [32,33,34▪▪].

THE OPTIC NERVE: MINIMUM DISTANCE BAND AND THREE-DIMENSIONAL IMAGING

Similar to the low-density commercially available BMO-MRW, good diagnostic ability can be achieved with a high-density research scan rim measurement, the minimum distance band (MDB). Both the high-density MDB and the low-density BMO-MRW parameters quantify neuroretinal rim tissue without a mathematically flat reference plane, and Fig. 1 [35] compares how these two parameters are calculated.

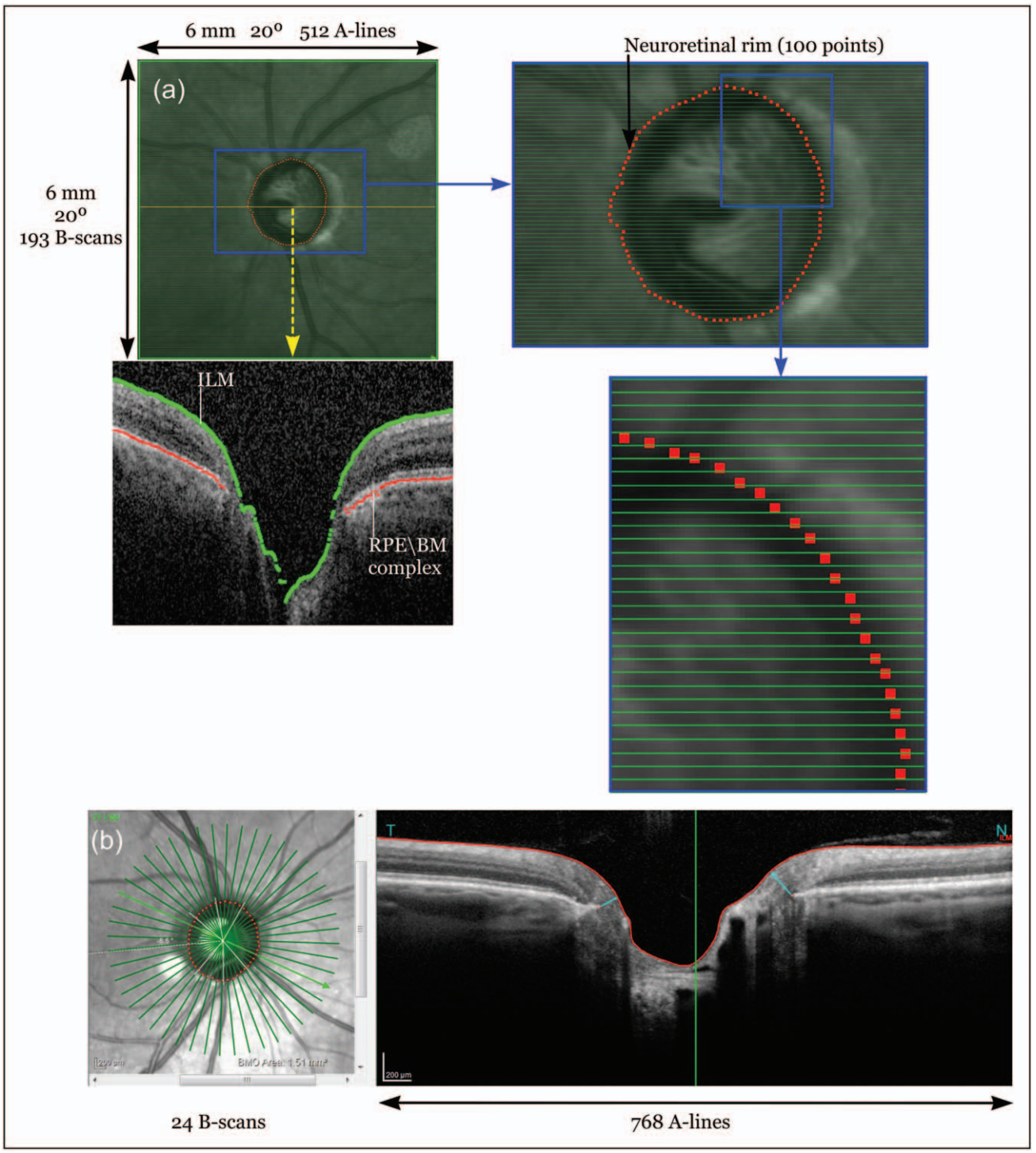

FIGURE 1. The minimum distance band volumetric high-density raster scan protocol compared with the Bruch's membrane opening-minimum rim width radial scan protocol. In (a), the horizontal green lines represent the 193 raster lines, which are used to reconstruct the OCT disc margin (100 red points), defined as the RPE/BM border. The lower left image in (a) is an OCT B-scan at the position of the yellow line. It depicts the automated segmentation of the ILM and the RPE/BM complex. In (b), the 24 radial scan pattern of the BMO-MRW protocol is shown. The OCT disc margin is reconstructed at 48 positions (48 red points) and is defined as the BMO border. Reproduced with permission from [35]. BMO-MRW, Bruch's membrane opening-minimum rim width; OCT, optical coherence tomography; RPE/BM, retinal pigment epithelium/Bruchs membrane.

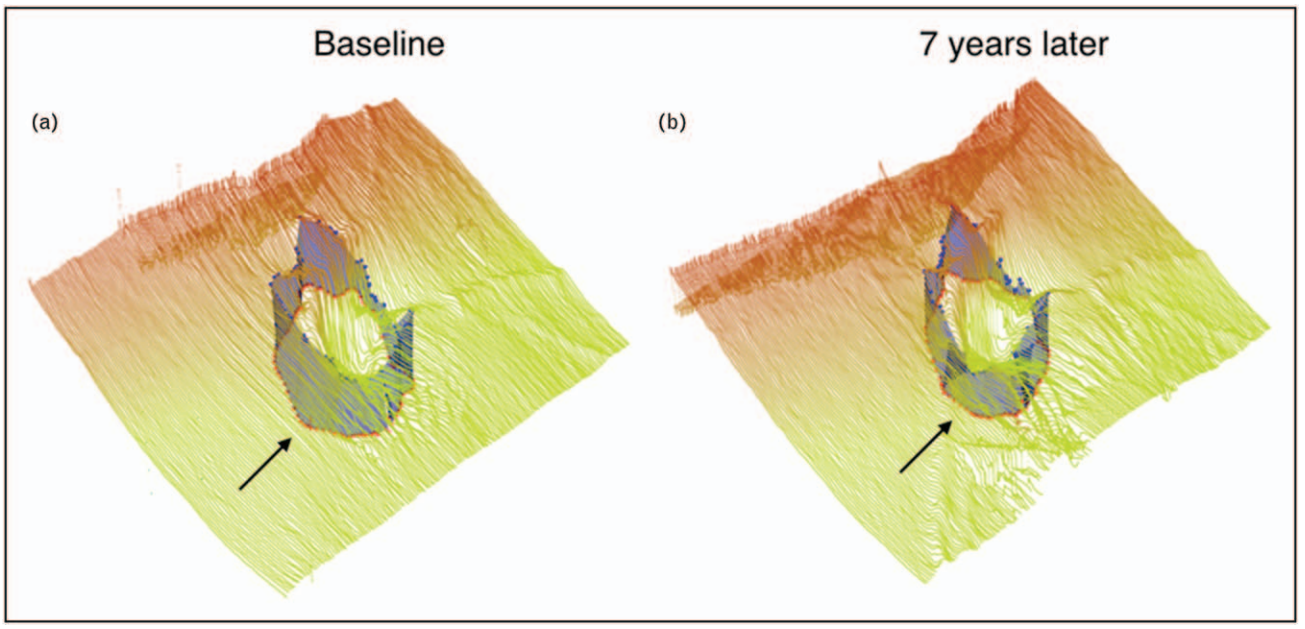

FIGURE 2. Example of the three-dimensional neuroretinal rim thickness (minimum distance band) of a progressing left eye imaged with Spectralis spectral-domain OCT: (a) baseline global minimum distance band thickness of the left eye and (b) global minimum distance band thickness 7 years later. The black arrows indicate the progressive focal MDB neuroretinal rim thinning (b) compared with baseline measurement (a). Reproduced with permission from [37▪▪]. MDB, minimum distance band.

The scan protocols are different as the MDB uses a high-density 193-line raster scan and the BMO-MRW uses a low-density 24-line radial scan. Although both define the inner rim border as the cup surface, the outer rim border is different. For the MDB, the disc border is the retinal pigment epithelium/Bruchs membrane (RPE/BM) complex. For the BMO-MRW, the disc border is the BMO. Studies have shown that the MDB rim thickness in 3D space has the same or better diagnostic ability compared with both RNFL thickness and 2D neuroretinal rim parameters [2,29,33,35]. Shieh *et al.* [29] demonstrated that glaucoma patients had significantly thinner MDB values in all quadrants and sectors, compared with control participants ($P < 0.0001$). The best AUROC values for glaucoma and early glaucoma patients were the overall global (AUROC 0.969; 0.952), the inferior quadrant (AUROC 0.966; 0.949), and the inferotemporal sector (AUROC 0.966; 0.944) [29].

An advantage of high-density MDB rim measurements in 3D space is that more data is obtained, resulting in fewer unusable scans. Park *et al.* [36▪▪] showed that the 3D MDB thickness parameter has only 15.8% unusable scans, compared with 2D RNFL thickness with 61.7% unusable scans.

Moreover, a longitudinal study demonstrated that MDB rim thickness can detect glaucomatous structural damage 1–2 years earlier than current clinical tests (i.e. RNFL thickness and disc photos) [37▪▪]. This was demonstrated in a cohort of 124 OAG patients followed for an average of 5 years [37▪▪]. An example from this article [37▪▪] shows an OAG patient who had progressive MDB thinning over a 7-year period (Fig. 2). For an irreversible blinding disease like glaucoma, treatment initiated 1–2 years earlier has invaluable impact and public health significance.

AROUND THE OPTIC NERVE: PERIPAPILLARY RETINAL VOLUME THREE-DIMENSIONAL IMAGING

One of the main problems with RNFL measurements is that segmentation of the posterior RNFL border is more inaccurate in glaucoma patients, whose RNFL is less reflective. A possible solution is peripapillary retinal thickness maps, whose posterior border (i.e. the RPE) is easier to accurately segment. This concept was published by Yi *et al.* [38], who showed examples where peripapillary retinal thickness maps revealed arcuate defects not seen on RNFL thickness maps (Fig. 3) [38]. Peripapillary retinal thickness measurements are different than macular retinal thickness maps, which are available in commercially available software. With this concept of peripapillary retinal thickness measurements, Simavli *et al.* [25] used the commercially available ETDRS (Early

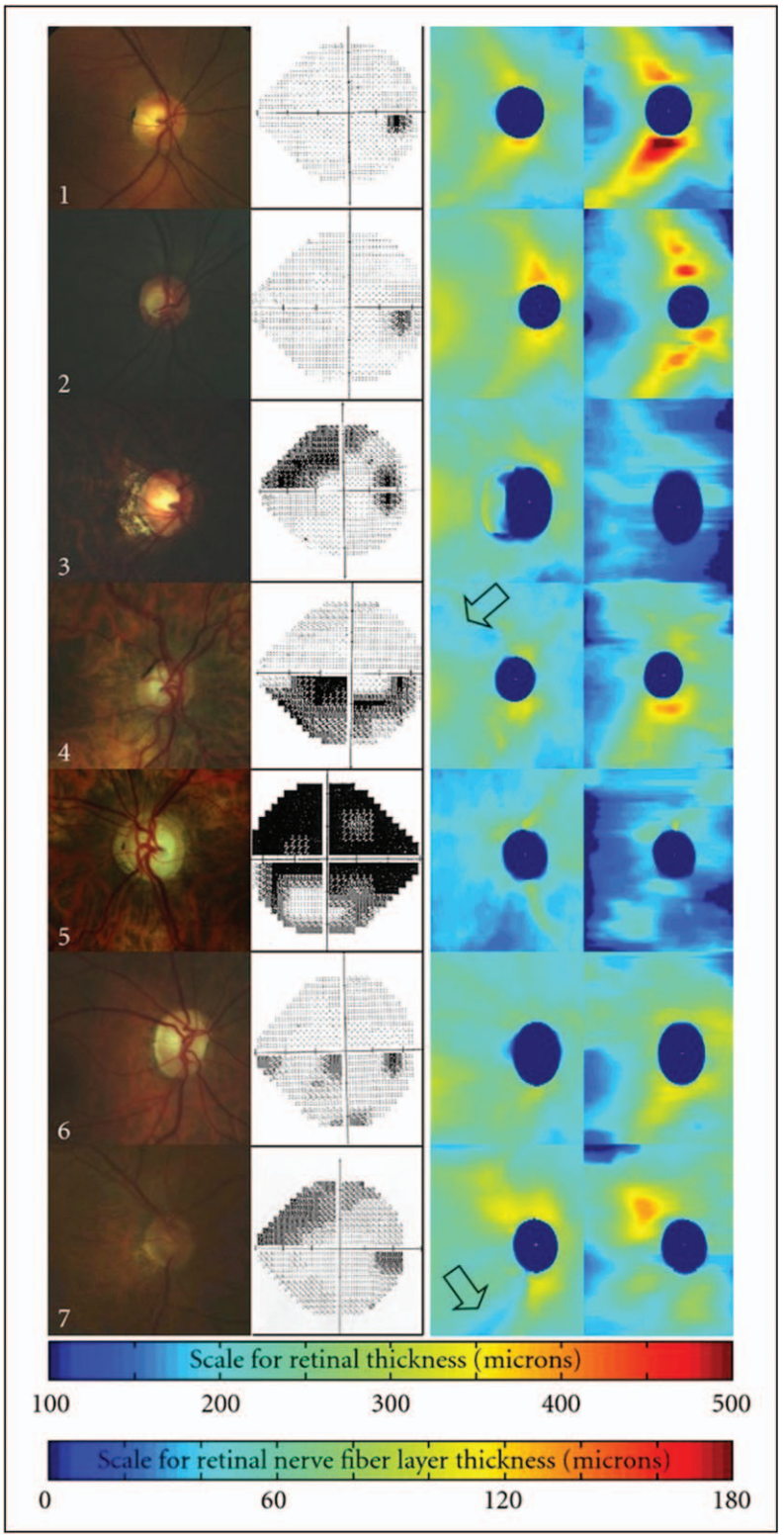

FIGURE 3. Spectral domain optical coherence tomography retinal thickness and retinal nerve fiber layer thickness peripapillary maps in normal (no. 1–2) and glaucoma (no. 3–7) patients. First column: disc photos, second column: visual fields, third column: RT maps, and fourth column: RNFL thickness maps. The thickness scales are seen as the bottom two color bars. The RT map scale ranges from 0 to 500 μm, and the RNFL thickness scale ranges from 0 to 180 μm. Visualization of classic glaucomatous arcuate defects is better seen in RT maps (arrows) than RNFL maps for eyes numbered 4 and 7. Reproduced with permission from [38]. RFNL, retinal nerve fiber layer; RT, retinal thickness.

Treatment Diabetic Retinopathy Study) scan circles and centered it over the optic nerve instead of the fovea. For all tested circumpapillary annuli sizes, the peripapillary retina was thinner in OAG patients for all quadrants, compared with normal participants, and best diagnostic regions were located inferiorly [25].

Furthermore, two other studies showed that peripapillary retinal volume measurements [26▪▪,39] have excellent performance as a diagnostic tool to detect glaucoma as retinal volume is lower in OAG patients compared with normal patients. The first study used ETDRS scan circles in commercially available software packages and showed that best retinal volume parameters had similar diagnostic ability compared with best RNFL thickness parameters [39]. The second study used research software, specifically designed for glaucoma diagnosis [26▪▪], to calculate 3D peripapillary retinal volume. In this article [26▪▪], customizable scan-circle sizes were used to create different-annuli sizes to evaluate eight possible peripapillary total retinal parameters. The best parameter found was the retinal volume – 2.5–3.5, which is the volumetric annular region centered on the optic nerve, whose inner border is 2.5 mm and outer border is 3.5 mm. A recurring theme when comparing 3D measurements with 2D RNFL thickness scans is that 3D retinal volume measurements had lower artifact rates than 2D RNFL thickness scans (6 vs. 32.2%, $P < 0.0001$) [26▪▪].

THE MACULA: GANGLION CELL COMPLEX VOLUME AND THREE-DIMENSIONAL IMAGING

The ganglion cell complex (GCC) constitutes the three innermost retinal layers: the RNFL, the ganglion cell layer (GCL), and the inner plexiform layer (IPL). Although commercial software calculates GCC thickness, future parameters may include GCC volume [40]. Verticchio *et al.* implemented six different-sized annuli (Fig. 4) and evaluated 12 possible macular parameters. This study demonstrated that the best 3D macular parameter (GCC-volume-34, which is the volumetric annular region centered on the macula, whose inner border is 3 mm and outer border is 4 mm) had the same or better diagnostic capability as the 2D RNFL thickness parameter [40].

OPTICAL COHERENCE TOMOGRAPHY: UNDERSTANDING THE MECHANICAL AND VASCULAR THEORIES OF GLAUCOMA

There are two main theories of glaucoma pathophysiology: the mechanical theory and the vascular theory [41]. The mechanical theory focuses on changes in the lamina cribrosa, which can be visualized with SD-OCT and SS-OCT. In an SS-OCT review, Takusagawa *et al.* concluded that imaging of the anterior laminar structures is more reliable than imaging of the posterior lamina, whose border is not consistently seen. With progressive glaucoma, there is posterior migration of

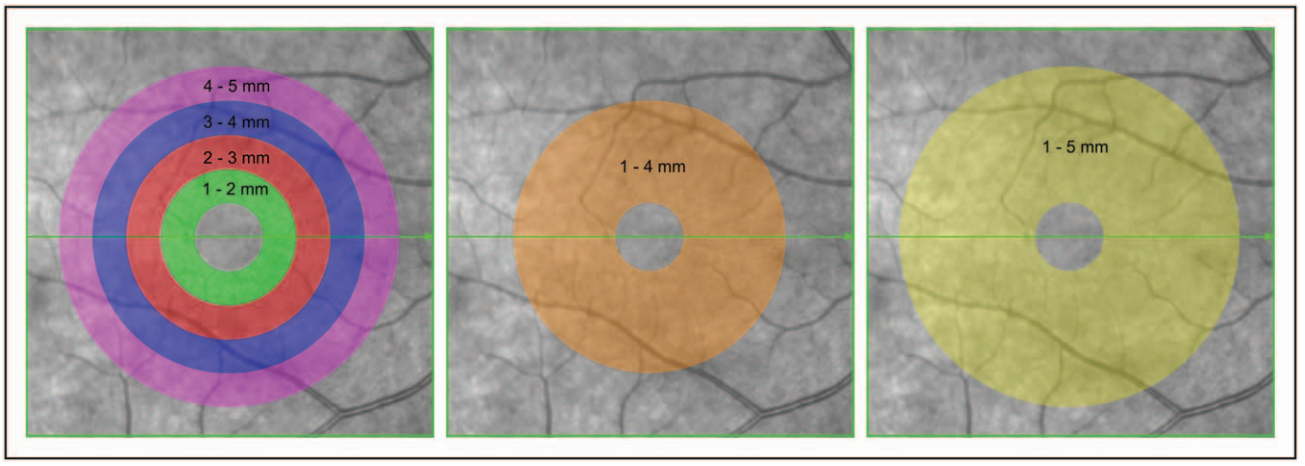

FIGURE 4. The six different-sized annuli, which were used to calculate the macular parameters, are depicted and superimposed on an en face spectral domain optical coherence tomography macular image. This figure specifically explains the terminology used for the six macular volume (M-volume) annuli: the smallest annulus (M-volume-12) is delimited by circles of diameters 1.00 and 2.00 mm (green area in the left image); the second annulus (M-volume-23) by circles of diameters 2.00 and 3.00 mm (red area in the left image); the third annulus (M-volume-34) by 3.00 and 4.00 mm (blue area in the left image); the fourth annulus (M-volume-45) by 4.00 and 5.00 mm (violet area in the left image); the fifth annulus (M-volume-14) by 1.00 and 4.00 mm (orange area in the center image), and the largest annulus (M-volume-15) by 1.00 and 5.00 mm (yellow area in the right image). Reproduced with permission from [40].

the anterior laminar insertions, with increased thinning and posterior curvature of the lamina. With glaucoma, focal laminar defects are more common, lamina microarchitecture re-models, and laminar pore size is more variable [12▪▪].

The vascular theory focuses on blood flow abnormalities and vasospasm as a cause of optic nerve damage. A review of OCTA for glaucoma reported capillary-vessel density decreases within the peripapillary nerve fiber layer and the macula in patients with glaucoma [18▪▪]. They also concluded there is a moderate-to-strong association between peripapillary OCTA vessel density and visual field defects and described similar discriminatory ability between peripapillary OCTA and OCT RNFL thickness. Studies reported areas without any visible vascular network in the choroidal or deep layer microvasculature in at least half of glaucoma patients. Lower peripapillary and macular vessel-density and choroidal microvasculature dropout are associated with faster rates of disease progression [18▪▪].

CONCLUSION

Newer 3D glaucoma parameters, which quantify volumetric data from high-density OCT volume scans may have equal or better diagnostic capability for detecting glaucomatous structural damage compared with the most commonly used, commercially available RNFL thickness parameter. The future of glaucoma OCT imaging should fully utilize SD-OCT's and SS-OCT's imaging abilities by presenting the physician with more data (i.e. 3D data instead of 2D data) and fewer imaging artifacts (i.e. fewer unusable scans). More data with fewer artifacts would not only improve clinical glaucoma care but also help us to better understand the mechanical and vascular theories of glaucoma.

Acknowledgements

None.

Financial support and sponsorship

Research supported in part by Fidelity Charitable Fund.

Conflicts of interest

There are no conflicts of interest.

REFERENCES AND RECOMMENDED READING

Papers of particular interest, published within the annual period of review, have been highlighted as:

- ▪ of special interest
- ▪▪ of outstanding interest

1. Huang D, Swanson EA, Lin CP, *et al.* Optical coherence tomography. Science 1991; 254:1178–1181.
2. Chen TC. Spectral domain optical coherence tomography in glaucoma: qualitative and quantitative analysis of the optic nerve head and retinal nerve fiber layer (an AOS thesis). Trans Am Ophthalmol Soc 2009; 107: 254–281.
3. Chen TC, Hoguet A, Junk AK, *et al.* Spectral-domain OCT: helping the clinician diagnose glaucoma: a report by the American Academy of Ophthalmology. Ophthalmology 2018; 125:1817–1827.
4. Mwanza JC, Warren JL, Budenz DL. Utility of combining spectral domain optical coherence tomography structural parameters for the diagnosis of early glaucoma: a mini-review. Eye Vis (Lond) 2018; 5:9.
5. Sharma R, Sharma A, Arora T, *et al.* Application of anterior segment optical coherence tomography in glaucoma. Surv Ophthalmol 2014; 59:311–327.
6. Chinn SR, Swanson EA, Fujimoto JG. Optical coherence tomography using a frequency-tunable optical source. Opt Lett 1997; 22:340–342.
7. Choma M, Sarunic M, Yang C, Izatt J. Sensitivity advantage of swept source and Fourier domain optical coherence tomography. Opt Express 2003; 11:2183–2189.
8. Yasuno Y, Madjarova VD, Makita S, *et al.* Three-dimensional and high-speed swept-source optical coherence tomography for in vivo investigation of human anterior eye segments. Opt Express 2005; 13:10652–10664.
9. Yun S, Tearney G, de Boer J, *et al.* High-speed optical frequency-domain imaging. Opt Express 2003; 11:2953–2963.
10. Lim H, Mujat M, Kerbage C, *et al.* High-speed imaging of human retina in vivo with swept-source optical coherence tomography. Opt Express 2006; 14:12902–12908.
11. de Bruin DM, Burnes DL, Loewenstein J, *et al.* In vivo three-dimensional imaging of neovascular age-related macular degeneration using optical frequency domain imaging at 1050 nm. Invest Ophthalmol Vis Sci 2008; 49:4545–4552.
12. ▪▪ Takusagawa HL, Hoguet A, Junk AK, *et al.* Swept-Source OCT for evaluating the lamina cribrosa: a report by the American Academy of Ophthalmology. Ophthalmology 2019; 126:1315–1323.

In this American Academy of Ophthalmology literature review of 29 articles of swept-source optical coherence tomography (SS-OCT) and in-vivo imaging of the lamina cribrosa, the authors concluded that imaging of the anterior lamina is more reliable than imaging of the posterior lamina. In glaucomatous eyes, lamina cribrosa depth increases, and its anterior insertions appear to be more posteriorly located. With glaucoma, the lamina is thinner, is more curved, has more focal defects, and has more variable pore size.

13. Lavinsky F, Lavinsky D. Novel perspectives on swept-source optical coherence tomography. Int J Retina Vitreous 2016; 2:25.
14. Vira J, Marchese A, Singh RB, Agarwal A. Swept-source optical coherence tomography imaging of the retinochoroid and beyond. Expert Rev Med Devices 2020; 17:413–426.
15. ▪ Lopes FS, Matsubara I, Almeida I, *et al.* Structure-function relationships in glaucoma using enhanced depth imaging optical coherence tomography-derived parameters: a cross-sectional observational study. BMC Ophthalmol 2019; 19:52.

In this study, the authors use enhanced-depth imaging spectral-domain optical coherence tomography (EDI SD-OCT) to evaluate structural and functional correlations of laminar and prelaminar parameters in healthy participants and glaucoma patients with a wide range of disease stages. They found that prelaminar parameters, such as BMO-MRW, have better structure function correlations than the laminar parameters.

16. Dong ZM, Wollstein G, Wang B, Schuman JS. Adaptive optics optical coherence tomography in glaucoma. Prog Retin Eye Res 2017; 57:76–88.
17. Akyol E, Hagag AM, Sivaprasad S, Lotery AJ. Adaptive optics: principles and applications in ophthalmology. Eye (Lond) 2021; 35:244–264.
18. ▪▪ WuDunn D, Takusagawa HL, Sit AJ, *et al.* OCT angiography for the diagnosis of glaucoma: a report by the American Academy of Ophthalmology. Ophthalmology 2021; 128:1222–1235.

In this American Academy of Ophthalmology literature review of 75 articles on OCTA, OCTA was noted to be able to detect decreased capillary vessel density within the peripapillary nerve fiber layer and macula in patients with suspected glaucoma, preperimetric glaucoma and perimetric glaucoma.

19. White B, Pierce M, Nassif N, *et al.* In vivo dynamic human retinal blood flow imaging using ultra-high-speed spectral domain optical coherence tomography. Opt Express 2003; 11:3490–3497.
20. Rao HL, Pradhan ZS, Suh MH, *et al.* Optical Coherence Tomography Angiography in Glaucoma. J Glaucoma 2020; 29:312–321.
21. Spaide RF, Fujimoto JG, Waheed NK, *et al.* Optical coherence tomography angiography. Prog Retin Eye Res 2018; 64:1–55.
22. Yao X, Alam MN, Le D, *et al.* Quantitative optical coherence tomography angiography: a review. Exp Biol Med (Maywood) 2020; 245:301–312.
23. ▪ Weindler H, Spitzer MS, Schultheiß M, Kromer R. OCT angiography analysis of retinal vessel density in primary open-angle glaucoma with and without Tafluprost therapy. BMC Ophthalmol 2020; 20:444.

With the use of OCTA, this study demonstrates that tafluprost reduces IOP in patients with open-angle glaucoma (OAG) and increases the peripapillary flow density in all sectors.

24. Asrani S, Essaid L, Alder BD, Santiago-Turla C. Artifacts in spectral-domain optical coherence tomography measurements in glaucoma. JAMA Ophthalmol 2014; 132:396–402.

25. Simavli H, Que CJ, Akduman M, *et al.* Diagnostic capability of peripapillary retinal thickness in glaucoma using 3D volume scans. Am J Ophthalmol 2015; 159:545.e2–556.e2.

26. ■■ Liu Y, Jassim F, Braaf B, *et al.* Diagnostic capability of 3D peripapillary retinal volume for glaucoma using optical coherence tomography customized software. J Glaucoma 2019; 28:708–717.

Peripapillary retinal volume is a novel parameter for the evaluation of glaucoma patients. Prior literature [25,37■■] determined peripapillary retinal volume measurements by moving the Early Treatment Diabetic Retinopathy Study (ETDRS) macular grid, which has fixed-sized scan circles designed for the analysis of diabetic macular disease, over the optic nerve. In this article, Liu *et al.* introduces novel software, which not only measures RV around the optic nerve but also was specifically designed for glaucoma diagnosis, allowing for customizable scan circle sizes.

27. ■ Antar H, Tsikata E, Ratanawongphaibul K, *et al.* Analysis of neuroretinal rim by age, race, and sex using high-density 3-dimensional spectral-domain optical coherence tomography. J Glaucoma 2019; 28:979–988.

In this study, the authors show the effect of age, race, and sex on the high-density neuroretinal rim MDB parameter in normal eyes. It is important for clinicians to be aware of expected normal aging changes and racial variations of rim thickness, in order to better distinguish normal rim changes from glaucomatous changes.

28. Liu Y, Simavli H, Que CJ, *et al.* Patient characteristics associated with artifacts in Spectralis optical coherence tomography imaging of the retinal nerve fiber layer in glaucoma. Am J Ophthalmol 2015; 159:565.e2–576.e2.

29. Shieh E, Lee R, Que C, *et al.* Diagnostic performance of a novel three-dimensional neuroretinal rim parameter for glaucoma using high-density volume scans. Am J Ophthalmol 2016; 169:168–178.

30. Khoueir Z, Jassim F, Poon LY, *et al.* Diagnostic capability of peripapillary three-dimensional retinal nerve fiber layer volume for glaucoma using optical coherence tomography volume scans. Am J Ophthalmol 2017; 182:180–193.

31. ■■ Choi S, Jassim F, Tsikata E, *et al.* Artifact rates for 2D retinal nerve fiber layer thickness versus 3D retinal nerve fiber layer volume. Transl Vis Sci Technol 2020; 9:12.

This study is the first to show that 3D RNFL volume scans have fewer artifacts than 2D RNFL thickness scans. Fewer clinically significant artifacts were noted in 3D RNFL volume scans (7.5% of glaucomatous eyes and 0% of normal eyes) compared with 2D RNFL scans (58.5% of glaucomatous eyes and 14.7% of normal eyes). Therefore, compared with 2D RNFL scans, 3D RNFL volume scans less often require manual correction to obtain accurate measurements.

32. Chauhan BC, O'Leary N, AlMobarak FA, *et al.* Enhanced detection of open-angle glaucoma with an anatomically accurate optical coherence tomography-derived neuroretinal rim parameter. Ophthalmology 2013; 120:535–543.

33. Fan KC, Tsikata E, Khoueir Z, *et al.* Enhanced diagnostic capability for glaucoma of 3-dimensional versus 2-dimensional neuroretinal rim parameters using spectral domain optical coherence tomography. J Glaucoma 2017; 26:450–458.

34. ■■ Cho HK, Kee C. Rate of change in Bruch's membrane opening-minimum rim width and peripapillary RNFL in early normal tension glaucoma. J Clin Med 2020; 9:2321.

The authors report in this article that BMO-MRW may show a visible reduction rate of change (ROC) that is better than retinal nerve fiber layer (RNFL) thickness for detecting early progression in early normal tension glaucoma (NTG) patients, whose visual field may not show significant change.

35. Tsikata E, Lee R, Shieh E, *et al.* Comprehensive three-dimensional analysis of the neuroretinal rim in glaucoma using high-density spectral-domain optical coherence tomography volume scans. Invest Ophthalmol Vis Sci 2016; 57:5498–5508.

36. ■■ Park EA, Tsikata E, Lee JJ, *et al.* Artifact rates for 2D retinal nerve fiber layer thickness versus 3D neuroretinal rim thickness using spectral-domain optical coherence tomography. Transl Vis Sci Technol 2020; 9:10.

In this study, Park *et al.* showed that the high-density 3D neuroretinal rim MDB parameter has only 15.8% of unusable glaucoma scans that may require repeat scanning, compared with up to 61.7% of the commercially available 2D RNFL thickness scans that are potentially unusable and may require repeat scanning.

37. ■■ Ratanawongphaibul K, Tsikata E, Zemplenyi M, *et al.* Earlier detection of glaucoma progression using high-density 3-dimensional spectral-domain OCT optic nerve volume scans. Ophthalmol Glaucoma 2021; 4:604–616.

In this 5-year prospective longitudinal study of 124 glaucoma patients, a 3D SD-OCT neuororetinal rim parameter (i.e. MDB thickness) was able to detect glaucoma progression 1–2 years earlier than standard clinical structural tests (i.e. disc photography and RNFL thickness).

38. Yi K, Mujat M, Sun W, *et al.* Peripapillary retinal thickness maps in the evaluation of glaucoma patients: a novel concept. ISRN Ophthalmol 2011; 2011:146813.

39. Simavli H, Poon LY, Que CJ, *et al.* Diagnostic capability of peripapillary retinal volume measurements in glaucoma. J Glaucoma 2017; 26:592–601.

40. Verticchio Vercellin AC, Jassim F, Poon LY, *et al.* Diagnostic capability of three-dimensional macular parameters for glaucoma using optical coherence tomography volume scans. Invest Ophthalmol Vis Sci 2018; 59:4998–5010.

41. Flammer J, Orgül S, Costa VP, *et al.* The impact of ocular blood flow in glaucoma. Prog Retin Eye Res 2002; 21:359–393.

